JOURNAL OF GEOPHYSICAL RESEARCH, VOL. 101, NO. D21, PAGES 26,217–26,226, NOVEMBER 27, 1996

The storm of October 21-22, 1994, over Greece: Observations and model results

K. Lagouvardos, V. Kotroni, S. Dobricic, S. Nickovic, and G. Kallos
Department of Applied Physics, Laboratory of Meteorology, University of Athens, Athens, Greece

Abstract. During October 21, 1994, a cold front passed over Greece. This frontal passage provoked catastrophic floods and there were many casualties. Eleven deaths were reported during this event, nine of them inside the Greater Athens Area. Significant damages occurred in transportation telecommunication and energy supply networks, especially in the eastern part of the country. This paper reports on the simulations of the observed storm conducted by two numerical models: the Colorado State University-Regional Atmospheric Modelling System (CSU-RAMS) and the η-eta/National Meteorological Center (ETA/NMC) model. The intercomparison of results between a regional research-oriented model (RAMS) with an operational model (ETA/NMC) permitted to explore the capabilities and limitations of each one of them. RAMS was operated in a nonhydrostatic mode using explicit microphysics and grid nesting (two nests with 40- and 10-km horizontal grid interval) and provided results which compare favorably with observations, suggesting that the model can adequately represent the mesoscale structure of the system. ETA/NMC is a hydrostatic limited-area model using parameterization of large-scale and convective precipitation. It was operated with 25-km horizontal resolution and it forecasted successfully the major characteristics of the system but failed in reproducing quantitatively the precipitation pattern at the mesoscale.

1. Introduction

The numerical investigation of severe weather events such as cold frontal passages, squall lines, storms, and rapidly deepening cyclones has been the subject of numerous studies during the past years. The approaches in these studies were either the use of nonhydrostatic models [*Hemler et al.*, 1991; *Snook and Pielke*, 1995] or more often hydrostatic models [*Zhang and Fritsch*, 1986; *Ross*, 1987; *Whitaker et al.*, 1988; *Warner and Seaman*, 1990 among others]. For the case of hydrostatic models, successful simulations were reported when additional explicit moisture schemes [*Zhang et al.*, 1989; *Belair et al.*, 1994] and increased horizontal resolution [*Ducrocq and Bougeault*, 1995], were used.

In the frame of this study, simulations have been performed using the Regional Atmospheric Modeling System (RAMS) developed at Colorado State University and ASTER Division of Mission Research Corporation and the η-eta/National Meteorological Center (ETA/NMC) developed at Belgrade University and National Meteorological Center (NMC) Washington, D.C. These models were used to numerically investigate a severe mesoscale weather phenomenon which presented significant spatial variability of precipitation.

Paper number 96JD01385.
0148-0227/96/96JD-01385$09.00

During October 21, 1994, a cold front passed over Greece. This event was associated with heavy precipitation and floods in urban areas as well as in the countryside. Many regions experienced one of their worst floods recorded the last 20 years. One of the most affected areas was the Greater Athens Area (GAA) where nine out of the eleven reported deaths occurred. Significant damages occurred in the transportation, telecommunication, and energy networks, mainly in the eastern part of the country. In some areas the accumulated 24-hour precipitation exceeded 140 mm, while near the center of Athens (Nea Philadelfia station) the 24-hour precipitation exceeded 90 mm.

The aim of this paper is to address the following questions: (1) Can a hydrostatic operational model predict such an extreme weather phenomenon over an area characterized by complex topography? (2) How the simulations of a model using explicit microphysics compare with those of an operational model, using parameterization of large-scale and convective precipitation, and how can both models forecast the spatial distribution of the observed precipitation?

The description of the models used is presented in section 2, while the models setup for the specific case study is given in section 3. Section 4 gives an overview of the case study in synoptic and mesoscale, based on upper air and surface observations. Section 5 presents the discussion of the model results, while the final section is devoted to the conclusions.

2. Description of the Models

The Regional Atmospheric Modelling System (RAMS) is a merger of a nonhydrostatic cloud model [*Tripoli and Cotton*,

1982] and a hydrostatic mesoscale model [*Mahrer and Pielke*, 1977]. A general description of the model and its capacities is given by *Pielke et al.* [1992]. However, some RAMS features are summarized in the following: Two-way interactive nested grid structure [*Clark and Farley*, 1984];.terrain following coordinate surfaces with cartesian or polar stereographic horizontal coordinates; cloud microphysics parameterization at various levels of complexity; modified Kuo cumulus parameterization [*Tremback*, 1990]; radiative transfer parameterizations (short and longwave) through clear and cloudy atmospheres [*Chen and Cotton*, 1987]; various options for upper and lateral boundary conditions and for finite operators; and various levels of complexity for surface layer parameterization (soil layer moisture and temperature model, vegetation parameterization, etc.)[*McCumber and Pielke*, 1981; *Avissar and Mahrer*, 1988].

The ETA/NMC model [*Mesinger et al.*, 1988; *Janjic*, 1994] uses a unique "step-mountain" vertical coordinate, (η-eta), rather than the customary pressure or sigma (or hybrid) coordinate. This coordinate is defined by:

$$\eta = \frac{p - p_T}{p_s - p_T}\eta_s \quad where \quad \eta_s = \frac{p_{rf}(z_s) - p_T}{p_{rf}(0) - p_T}$$

Here p is pressure; the subscripts T and s stand for the top and the ground surface values of the model atmosphere, respectively; z is the geometric height and $p_{rf}(z)$ is a suitably defined reference pressure as a function of z.

The ETA system preserves the simplicity of the sigma system lower boundary condition and at the same time overcomes most of the problems that appear in regions with steep mountains in sigma models. Through the no-slip lower boundary condition and other features of the mountain modelling, the orographic blocking, channelling and splitting effects are represented in a quite feasible way. Some ETA/NMC features are summarized in the following: Representation of the model variables on an Arakawa *E*-grid system; use of η (ETA) as vertical coordinate, a generalization of σ-coordinates; use of a split-explicit time differencing scheme; use of the Mellor-Yamada [*Mellor and Yamada*, 1982] turbulence scheme (level 2 in the surface layer, level 2.5 otherwise); use of fourth-order diffusion scheme with diffusion coefficients dependent on the deformation and turbulent kinetic energy; application of the modified Betts-Miller deep and shallow convection schemes [*Betts and Miller*, 1986; *Janjic*, 1994]; and use of the NMC version of the Goddard Laboratory for Atmospheres radiation scheme (GLAS) with random interaction of clouds at various levels.

The ETA/NMC model became operational at the NMC Washington in 1993. It has also been used as either an operational or a research model at a number of other institutions and for a number of different geographical regions. The model has been successful in forecasting severe mesoscale features. For additional details on the performance of the model the reader is referred to work by *Janjic* [1994].

3. Model Initialization and Grid Configuration

3.1. RAMS Setup

For the present application, RAMS was initialized at 0000 UTC October 21, 1994, and the duration of the simulation was 36 hours. The nonhydrostatic version of the model is employed, using two nested grids: the outer with a mesh of 76x62 points and 40 km horizontal grid interval and the inner with 122x110 points and 10 km horizontal grid interval centered at 40° N latitude and 20° E longitude (Figure 1). Thirty levels following the topography were used on both grids, having a 80 m vertical spacing near the ground, stretching to 1 km at 6.5 km altitude and remaining constant up to 16.5 km. Apart from these settings, a rigid lid has been set at the model top boundary by constraining vertical velocity to be zero there. A soil layer has been used to predict the sensible and latent heat fluxes at the soil-atmosphere interface. Eleven soil levels have been used down to 50 cm below the surface. The lateral boundary conditions on the outer grid followed the Klemp-Lilly condition [*Klemp and Lilly*, 1978] with vertical average of the gravity wave propagation speed at the boundaries. The full microphysics scheme available in RAMS code has been used which activates the microphysical parameterization of rainwater, pristine ice,

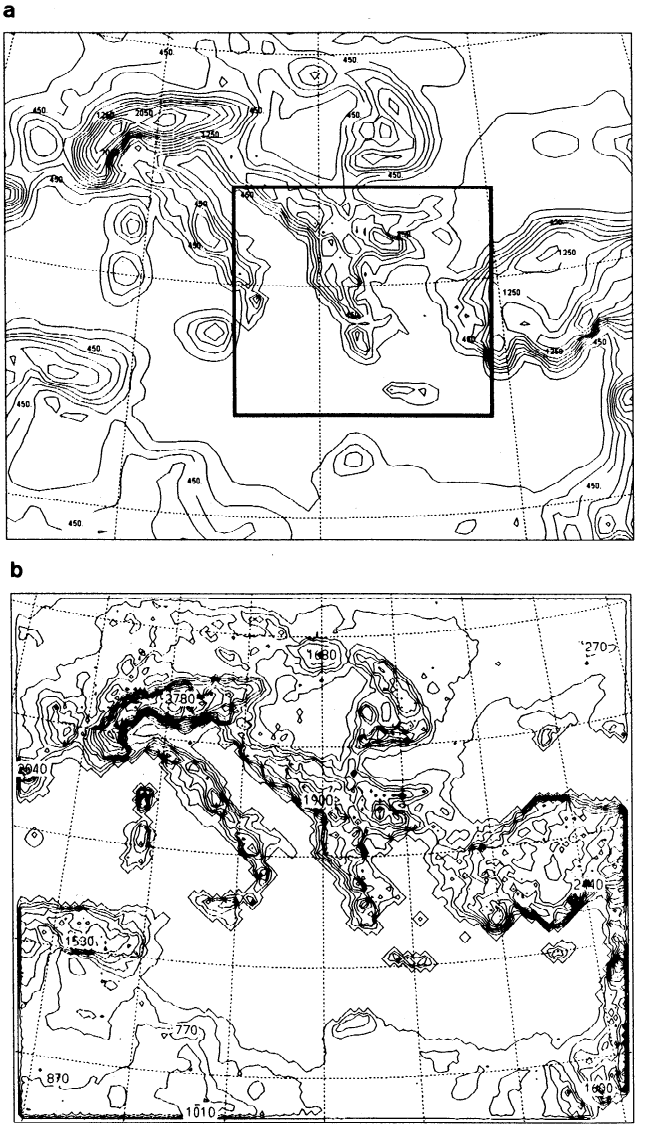

Figure 1. (a) Domain of RAMS model (the rectangle indicates the inner grid); (b) domain of η-eta (ETA) model. Topography is contoured every 200 m.

snow, and aggregates. Moreover, the cumulus parameterization options in RAMS has been employed.

The European Center for Meteorological Weather Forecasting (ECMWF) 1° gridded analysis files were used in order to initialize the model. The ECMWF data are objectively analyzed by the RAMS model on isentropic surfaces from which they are interpolated to the RAMS grids. These fields were used in order to nudge the lateral boundary region of the coarser grid every 6 hours. The ECMWF fields of the observed sea surface temperature (SST) and topography derived from a 5-min terrain data retrieved by the National Center for Atmospheric Research (NCAR) have been used for both grids.

3.2. ETA/NMC Setup

The model was initialized at 0000 UTC October 21, 1994, and the duration of the simulation was 36 hours. One nest has been used with a mesh of 61x121 points and 25-km horizontal grid interval centered at 40° N latitude and 20° E longitude. Thirty-two levels were used, with the lowest model level placed 90 m above the model topography or sea, having approximately 90-m vertical spacing at the lower level over the sea and 150 m over topography, stretching to 1.2 km at 16.5 km altitude. The initial fields were interpolated from ECMWF 1° gridded analysis files. As for RAMS, the ECMWF fields of the observed sea surface temperature and topography derived from a 5-min terrain data retrieved by NCAR have been used. The lateral boundaries are updated every 6 hours from the ECMWF analysis files.

4. Synoptic-Mesoscale Overview

At 0000 UTC October 21, 1994, a low center of 999 hPa was situated over the Gulf of Genoa. This cyclonic system propagated eastward, and 12 hours later it was centered over southern Italy and Sicily and has deepened to 996 hPa (Figure 2a). The cold front associated with this system was oriented north-south over the sea in the region southeast of Italy. An extended high-pressure system of 1040 hPa is also observed in central Russia. At the 850-hPa level warm advection is evident over the Mediterranean between Italy and Greece (Figure 2b), due to the low-level strong winds which were evident ahead of the cold front. A weak cold air intrusion from the northeast is also evident in the northern part of Greece. Six hours later, at 1800 UTC, the surface low has deepened to 994 hPa, while the cold front has progressed toward the Ionian Sea, between Italy and Greece and the western part of the Greek peninsula (Figure 2c). At the 850-hPa level, an important warm air advection is evident; note the position how the 16°C isotherm has been advected northward over a distance of about 350 km within 6 hours (Figure 2d).

Rawinsonde observations from Athens (Figure 3) at 1200 UTC October 21, 1994, indicated a near-saturated environment inside the whole troposphere. Wind observations at the lower levels are missing, but above 500 hPa the flow is relatively weak from southwest. The maximum wind of about 15 ms^{-1} is observed at the 150-hPa level. The total accumulated precipitation during a 24-hour period (from 0600 UTC October 21, to 0600 UTC October 22, 1994) is presented in Figure 4.

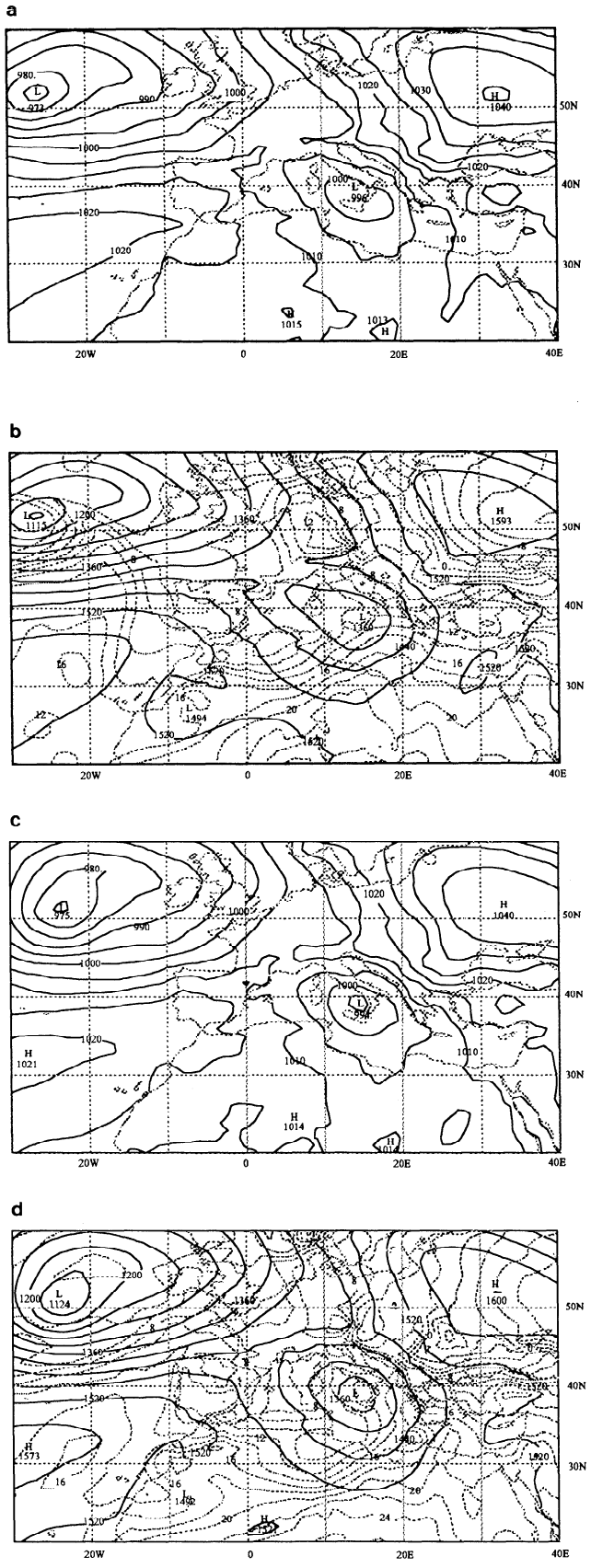

Figure 2. (a) Surface map at 1200 UTC October 21, 1994, with 5-hPa interval; (b) 850-hPa height (solid lines with 40-m interval) and temperature analysis (dashed lines with 2°C interval) at 1200 UTC October 21, 1994; Figure 2c as in Figure 2a but at 1800 UTC; Figure 2d as in Figure 2b but at 1800 UTC.

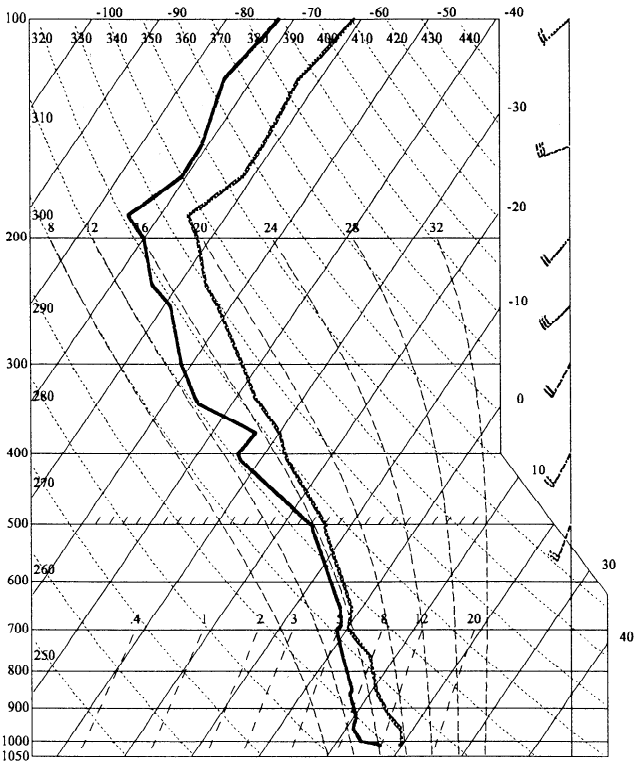

Figure 3. SkewT-logP diagram constructed from the sounding released at Athens airport at 1200 UTC, October 21, 1994. One full barb equals 5 ms^{-1} and a half barb equals 2.5 ms^{-1}.

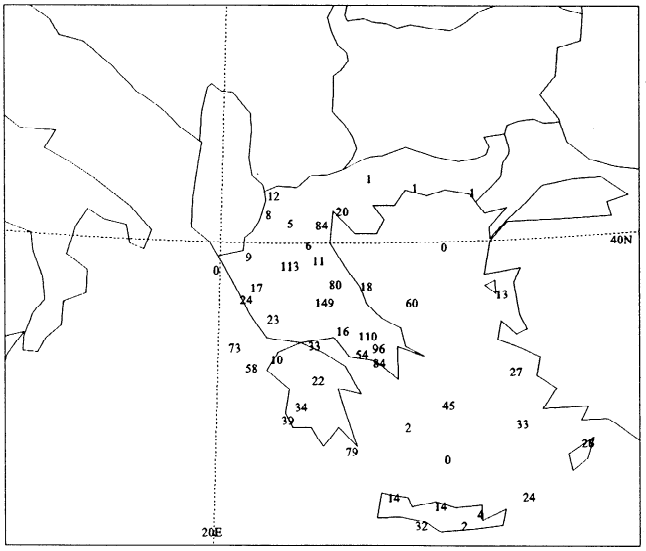

Figure 4. Total accumulated precipitation in millimeters from 0600 UTC October 21, to 0600 UTC October 22, 1994, reported by the surface stations.

Inspection of the observed precipitation pattern shows a band of heavy precipitation extending northward through Peloponnissos into the area of Athens. The maximum precipitation (96 mm) within GAA was reported in a station near the city center (Nea Philadelfia) where most of the damages occurred; the most important part of the precipitation accumulated in the time period from 1600 to 2000 UTC, October 21. In central Greece, a maximum of 149 mm is observed. In this region, important flooding has been reported. In northern Greece, two centers of heavy precipitation are observed with maximums of 113 mm in Trikala (east of the Pindos peninsula) and 84 mm in Katerini (east of Mount Olympus). Between these two regions of heavy precipitation a dry band is observed. The precipitation pattern shows a substantial spatial variability which will be investigated with the model simulations and especially the nesting capabilities of RAMS.

5. Model Simulations

5.1. RAMS results

Figure 5 shows the wind field of the outer grid of RAMS, at 1200 and 1800 UTC October 21, 1994. At 1200 UTC, at z=38 m (first model level), the frontal system is associated with a reduction of the wind intensity from 16 ms^{-1} to less than 10 ms^{-1} and a gradual wind veering of about 60° from south to southwest (Figure 5a). In the low levels the maximum winds are observed at about 1000 m with a maximum of 24 ms^{-1} south of Peloponnissos (not shown). Inspection of the 1800 UTC near surface wind pattern (Figure 5b) reveals a cyclonic circulation with its center situated over the straits between Italy and Albania. RAMS positions the low a little to the east from the position of the low shown in the ECMWF analysis (Figure 2c). The winds ahead of the front are from the south with a maximum intensity of about 18 ms^{-1}, and the frontal discontinuity is associated with a veering of about 60°. Behind this cold front, at a distance of about 400 km, a second frontal discontinuity associated with a wind veering is evident extending from Sicily down to the Libyan coasts. Inspection of the thermodynamic structure of this discontinuity revealed that this secondary front was very shallow (not shown). At 1000 m (Figure 5c) the wind veering associated with the cold front is also evident but it is less important than at surface (about 60°). The shallowness of the secondary front is also proved by the fact that no secondary discontinuity is evident in the wind field at 1000 m. One must also note the eastern-northeastern flow which is evident both near surface and at 1000 m over the Black Sea and the northern part of Greece. The discontinuity evident in the wind field pattern (Figures. 5a, 5b, 5c) over the northern Aegean Sea (following the 40° N latitude line) denotes the existence of a warm frontal surface. As a matter of fact, during the period of interest, the Greek Peninsula is affected by the warm sector of the low-pressure system.

Figure 6 shows the wind field of the inner grid of RAMS, near the surface, at 1800 UTC October 21, 1994. The wind veering associated with the frontal passage is clearly evident in this pattern. The wind intensity ahead of the front is of the order of 16 ms^{-1}, while behind the front the wind is less than 10 ms^{-1}. One must also note a channelling of the flow around the Greek Peninsula with strong eastern-southeastern winds over the northern Aegean Sea, directed toward the coast of eastern Greece, following a counterclockwise circulation associated with the low-pressure system depicted in Figure 2c.

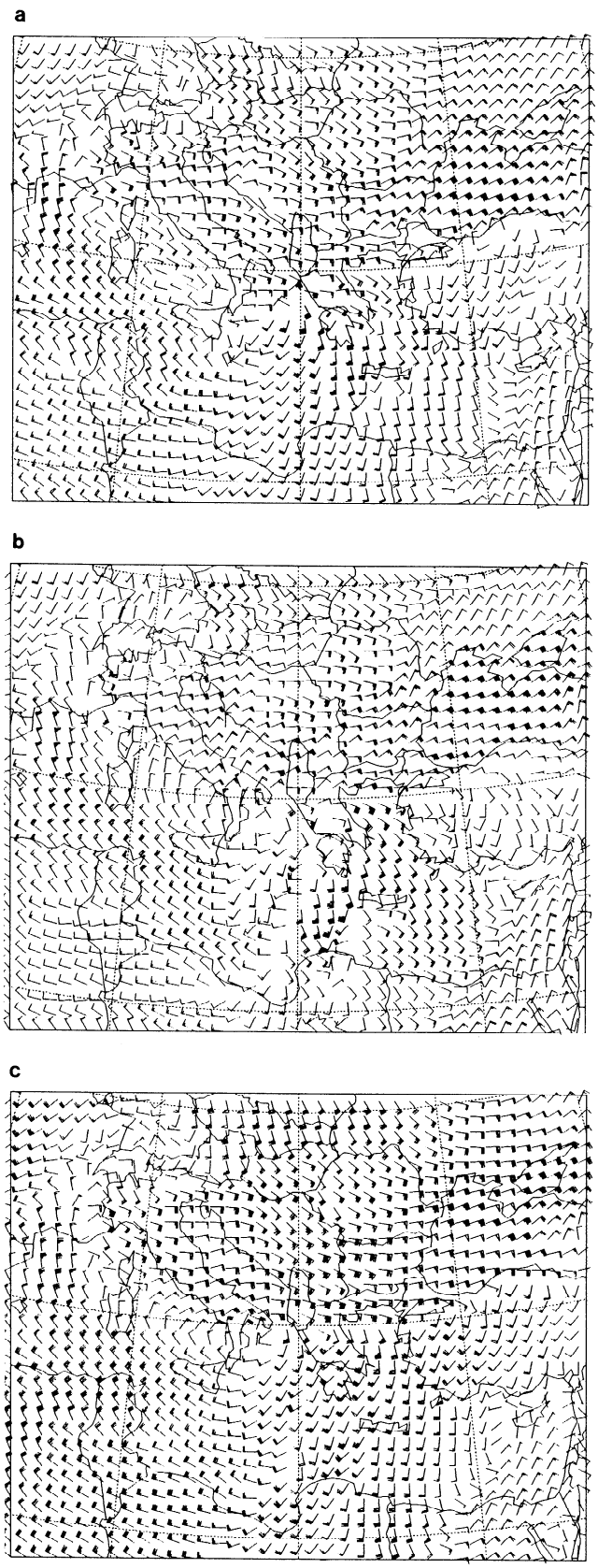

Figure 5. Horizontal cross section of RAMS outer grid (a) at z=38 m Above Ground Level (AGL) at 1200 UTC, (b) at z=38 m AGL at 1800 UTC, and (c) at z=1000 m AGL at 1800 UTC, October 21, 1994. Wind symbols are plotted every second grid point. One pennant equals 20 ms^{-1}, one barb 4 ms^{-1} and one half-barb 2 ms^{-1}.

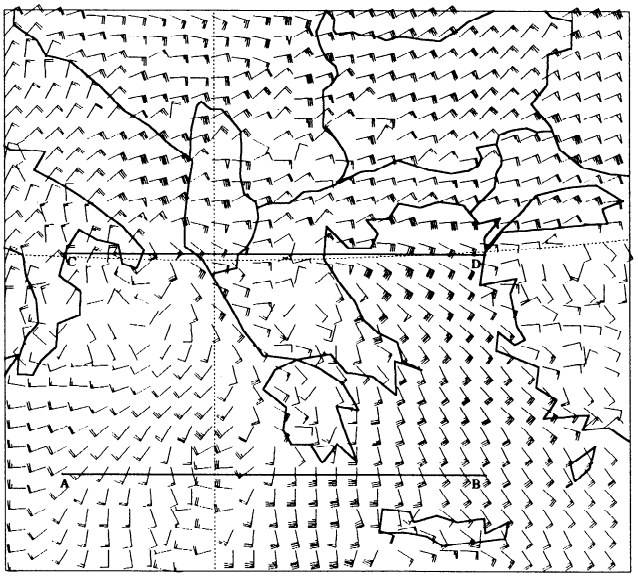

Figure 6. Horizontal cross section of RAMS inner grid at z=38 m AGL at 1800 UTC, October 21, 1994. Wind symbols are plotted every fourth grid point. One pennant equals 20 ms^{-1}, one barb 4 ms^{-1} and one half-barb 2 ms^{-1}. Lines AB (following the 35.54° N latitude) and CD (following the 40° N latitude) indicate the location of the vertical cross sections shown in Figures 7 and 8, respectively.

The detailed structure of the frontal system can be assessed by inspection of the dynamic and thermodynamic parameters inside the inner grid of RAMS. Figure 7 shows a vertical cross section of potential temperature, wind speed and vertical velocity in the region between Peloponnissos and Crete (over the sea). In the potential temperature field (Figure 7a) a horizontal gradient of 3K over a distance of 30 km is evident within the first 2.5 km of the atmosphere. At the height of about 10 km a second region of potential temperature horizontal gradient is evident which is associated with the presence of an upper level jet as this can be seen in Figure 7b. The maximum of this upper level jet is located at 10 km, exceeding 30 ms^{-1}. A second feature which can be depicted from Figure 7b is a well-defined low-level jet ahead of the frontal discontinuity, with a maximum exceeding 24 ms^{-1} at a height of about 700 m and a horizontal extension of about 350 km. This jet conveys warm and moist air from the marine boundary layer feeding the system with enough moisture to sustain heavy precipitation. Both upper and low-level jets have a south-north orientation coming from 200° sector. Behind the front the wind weakens at values of about 8 ms^{-1}. This structure of the thermodynamic and dynamic parameters (potential temperature horizontal gradient, low-level jet characteristics) is common for midlatitude cold fronts as these have been described by several observational studies [*Browning and Pardoe*, 1973; *Hobbs et al.*, 1980; *Thorpe and Clough*, 1991; *Kotroni and Lagouvardos*, 1993; *Kotroni et al.*, 1994].

The vertical velocity field is shown in Figure 7c. Positive values (indicating ascending motions) are evident just ahead of the frontal discontinuity. This region of ascending motions is very narrow and extends vertically up to the tropopause with a

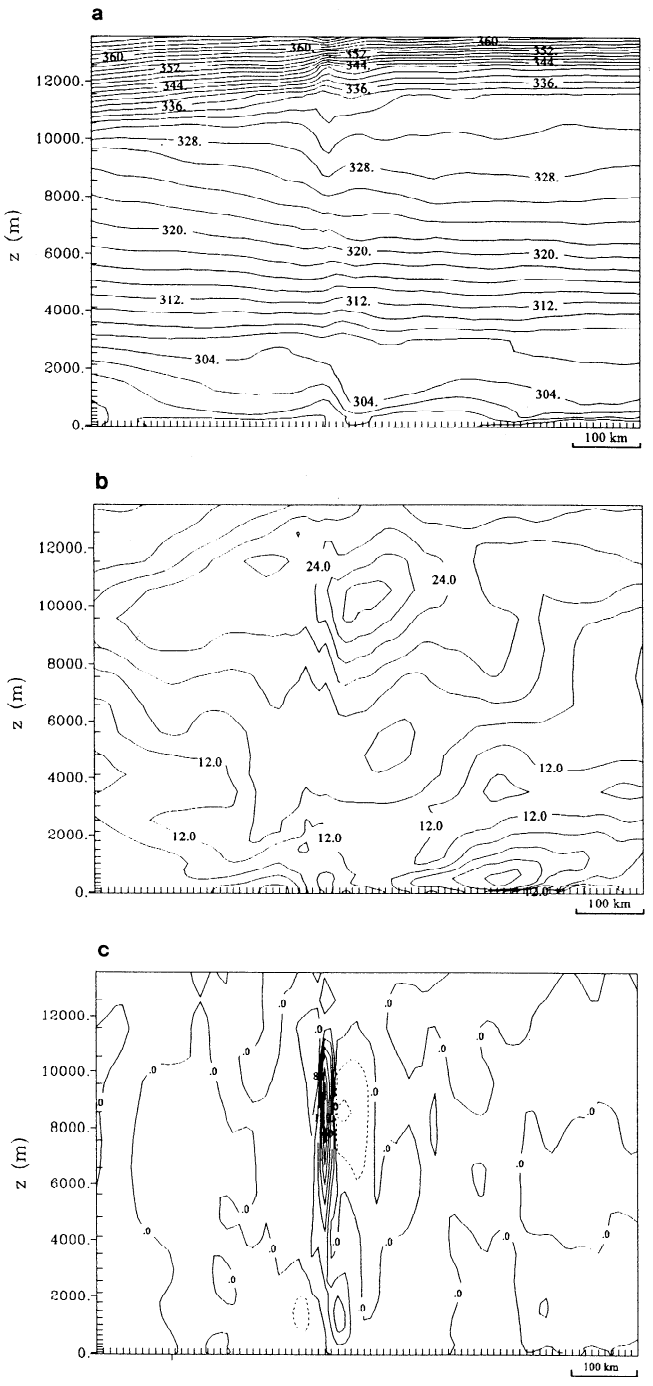

Figure 7. Vertical cross sections of RAMS inner grid at 1800 UTC October 21, 1994, of (a) potential temperature (at 2K interval), (b) wind speed (at 3 ms^{-1} interval), and (c) vertical velocity (at 20 cms^{-1} interval, negative values are dashed) following line AB on Figure 6.

maximum of 130 cms^{-1} located at 8.5 km. The maximum of the upward motion in the low levels is 50 cms^{-1} at a height of about 1000 m. Negative values (indicating subsidence) are evident in the cold sector; these subsiding motions are weaker with an absolute maximum of 20 cms^{-1}. It seems that the downdraft feeds the area behind the front with relatively cold air which propagating eastward acts as a density current and forces the warm and moist air to be lifted ahead of the frontal discontinuity. The downward motions evident at about 8 km could be associated to the circulation around the upper level jet evident in Figure 7b.

In order to study the flow over the main Greek Peninsula during this event, vertical cross sections in the region following the 40° latitude are presented in Figure 8. In the *u*-component of the wind field (Figure 8a), a strong eastern inflow is evident in the low-levels corresponding to the wind flow depicted in Figure 6. This inflow is relatively strong with a maximum of 24 ms^{-1} below 1000 m height just in front of the mountain barrier. The presence of this barrier contributes to the development of strong updrafts (Figure 8b) extending up to 12 km and presenting a maximum value of 6 ms^{-1} at the midtropospheric layers.

At this point the precipitation patterns should be discussed. Figure 9 presents the 24-hour accumulated precipitation field from 0600 UTC October 21, 1994, to 0600 UTC October 22, 1994, for the inner grid, predicted by RAMS using the detailed cloud microphysics parameterization. A band of heavy precipitation is observed in southern Greece, extending

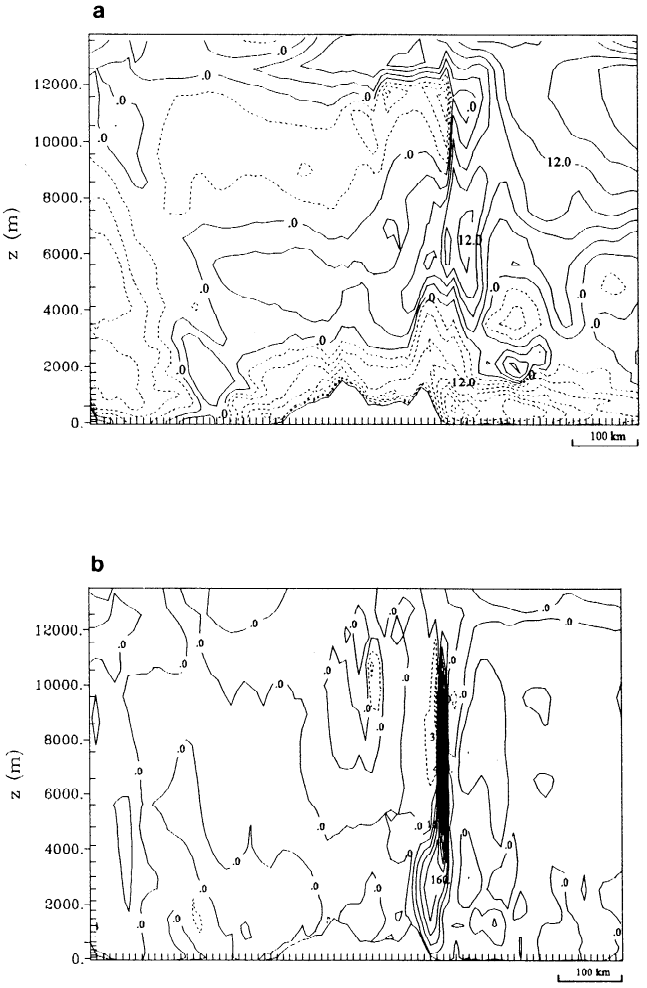

Figure 8. Vertical cross sections of RAMS inner grid, at 1800 UTC October 21, 1994, of (a) west-east wind component (at 3 ms^{-1} interval, negative values are dashed), and (b) vertical velocity (at 40 cms^{-1} interval, negative values are dashed) following line CD on Figure 6.

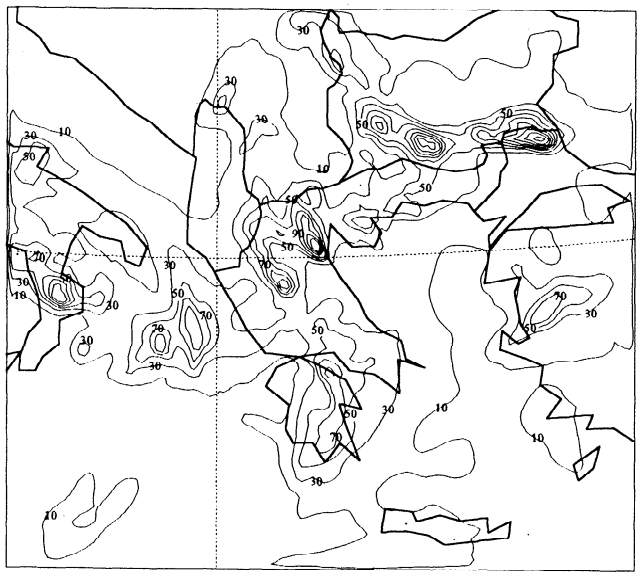

Figure 9. RAMS inner grid forecasted total accumulated precipitation from 0600 UTC October 21, to 0600 UTC, October 22, 1994 (contour interval of 20 mm).

northward through the south coasts of Peloponnissos into the region of Athens. The model failed to reproduce the spatial variability of precipitation within the region of Athens, giving values close to 50 mm, while the observed accumulated precipitation was varying from 54 to 96 mm (Figure 4). This must be partly due to the horizontal grid resolution used. It should be noted that the three measuring stations within the Athens area are spaced less than 10 km, representing phenomena of a scale much smaller than those which can be resolved by the model with the specific settings. Heavy precipitation is also predicted by RAMS over the Ionian Sea (west from the Greek Peninsula). Precipitation records do not exist over the sea, except the precipitation recorded at one of the most western surface stations, which measured 73 mm (Figure 4). Farther north, at about 40° N latitude, two cores of heavy precipitation were predicted, separated by a narrow dry zone. This feature predicted by RAMS, qualitatively compares favorably with the observations, predicting well the approximate position and orientation of the precipitation maxima. Nevertheless the model overpredicted the precipitation amount, giving maxima of 170 and 120 mm in the two regions of heavy precipitation, compared to the 83 and 113 mm accumulated precipitation recorded by the surface stations at the same areas. Between these two regions of heavy precipitation, a dry zone has been predicted characterized by precipitation amounts of about 30 mm which consists of an overestimation compared to the 5, 6, and 11 mm recorded within the dry band (Figure 4). One must also note that this region of heavy predicted and observed precipitation over northern Greece corresponds with the region characterized by strong inflow from northern Aegean Sea (Figures 6 and 8a) and deep updrafts (Figure 8b). One must note that south of these heavy precipitation regions in central Greece there is a region of heavy reported precipitation (149 mm, Figure 4) which the model failed to produce. Concerning the comparison between observed and predicted precipitation amounts, one should note that especially in convective situations, the spatial and temporal variability of the precipitation field is very difficult to be objectively analyzed by a sparse rain gauge network data. Lack of precipitation data from the neighbouring countries (Bulgaria, Turkey), prohibits further comparison.

5.2. ETA/NMC Results

The October 21, 1994, 1800 UTC ETA/NMC forecast of near surface winds (at $z \approx 130$ m) shows the cyclonic position (Figure 10a) to be over southern Italy, close to the ECMWF analysis position (Figure 2c). The predicted field shows similar

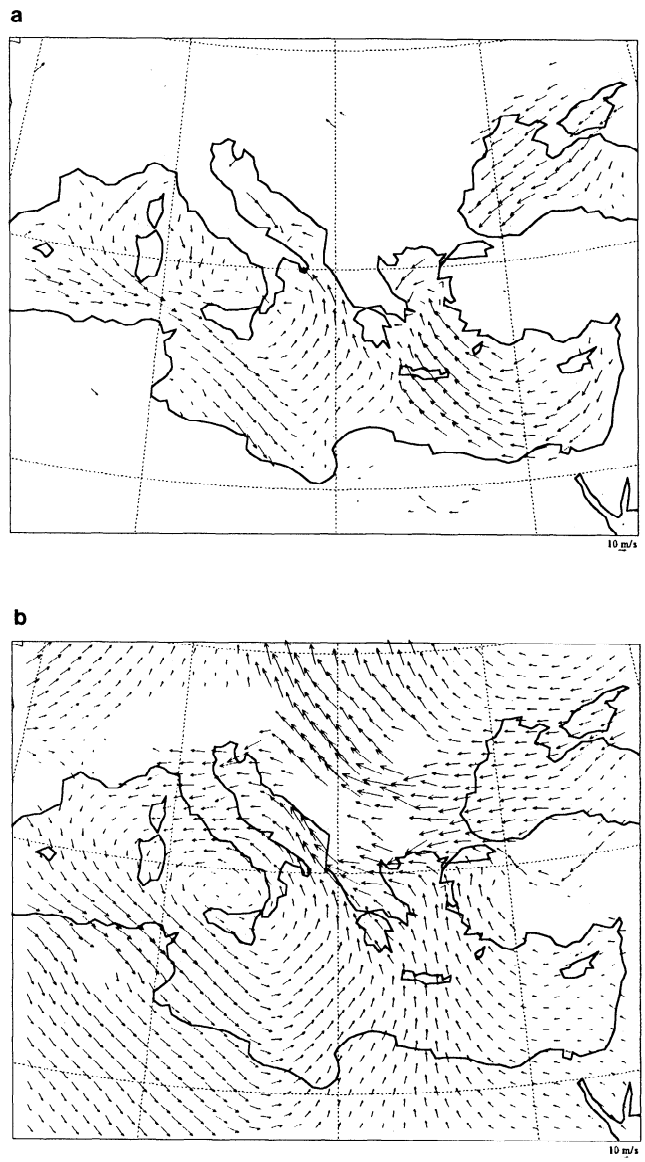

Figure 10. Horizontal cross section of ETA/NMC wind field at (a) z=130 m MSL (above Mean Sea Level) and (b) z=800 m MSL, at 1800 UTC, October 21, 1994. Wind symbols are plotted every other grid point.

characteristics with the RAMS predicted outer grid wind field (Figure 5a). The gradual wind veering associated with the frontal discontinuity is obvious south of Peloponnissos, while the second discontinuity behind this cold front at a distance of about 400 km, depicted in RAMS forecast (Figure 5a), is also evident. An important feature evident in the 800-m wind pattern (Figure 10b) is the strong southeastern inflow over the northern Aegean Sea and the strong eastern flow over the Black Sea directed toward northern Greece.

The main paths of air masses originating from different atmospheric layers can be investigated through inspection of the trajectories predicted by ETA/NMC model (Figure 11). For this calculation a run starting at 0000 UTC October 20, 1994, has been performed. The pattern presents the resulting trajectories at 1800 UTC, October 21, 1994. The trajectories indicate the following: (1) Air masses originating from the Sahara at a height of about 1.5 km (trajectories 1-5 in Figure 11) are inflowing over southern Greece and the Aegean Sea and at the same time they are lifted over the central part of Greece. (2) Air masses originating from the north-northeastern African Coast at a height of about 150 m (trajectories 6-10 in Figure 11) inflow the Aegean Sea from the east (through the region east of Crete and west of the Turkish Coast). (3) Air masses originating from the eastern Black Sea at a height of 150 m (trajectories 11-13 in Figure 11) inflow the northern Greece and northern Aegean Sea through the region of Dardanelles straits.

The 24-hour accumulated precipitation field from 0600 UTC October 21, 1994, to 0600 UTC October 22, 1994, forecasted by ETA/NMC is presented in Figure 12. A V-shaped band of precipitation exceeding 30 mm is observed from southern Italy down to Peloponnissos and then up to central Aegean Sea and the west coast of Turkey. The maximum predicted precipitation (91 mm) is over south Peloponnissos conforming with the RAMS predicted field and with the observed precipitation recorded in the area (79 mm, Figure 4). Comparing the precipitation patterns over northern Greece (Figure 9 and Figure 12) it should be noted that the ETA/NMC was credible, providing a reasonable position of the two regions of precipitation separated by the dry region aforementioned (when discussing the observations and RAMS results). The major shortcoming was that the amounts of precipitation were underestimated (40 mm) compared to the observations.

6. Conclusions

An extreme precipitation event over Greece has been simulated using two different numerical models. The aim of the study was to investigate the capability of RAMS to reproduce the spatial variability of precipitation at mesoscale as well as to compare these results with a hydrostatic operational model predictions of such an extreme weather phenomenon. This event was ideal to meet the scopes of this study since it was associated with heavy precipitation presenting significant mesoscale variability. Both models have been initialized with 1° ECMWF gridded analysis files. The horizontal grid size has been set to 40 and 10 km for the outer and the inner nest of RAMS, respectively, and 25 km for ETA/NMC.

The RAMS model simulation provided a complete description of the mesoscale features of the observed event. A squall line structure has been resolved over the sea south of Peloponnissos which was characterized by a strong temperature gradient and a low-level jet confined within the first 2 kilometers of the atmosphere. Strong updrafts were also predicted just ahead of the squall line. The ETA/NMC trajectories provided an idea on the origin of air masses feeding the analyzed system. Trajectories starting at about 1500 m show that air masses originating from the northern coast of Africa feed the system with moist and warm air resulting in strong updrafts over southern Greece. Air masses originating from the eastern

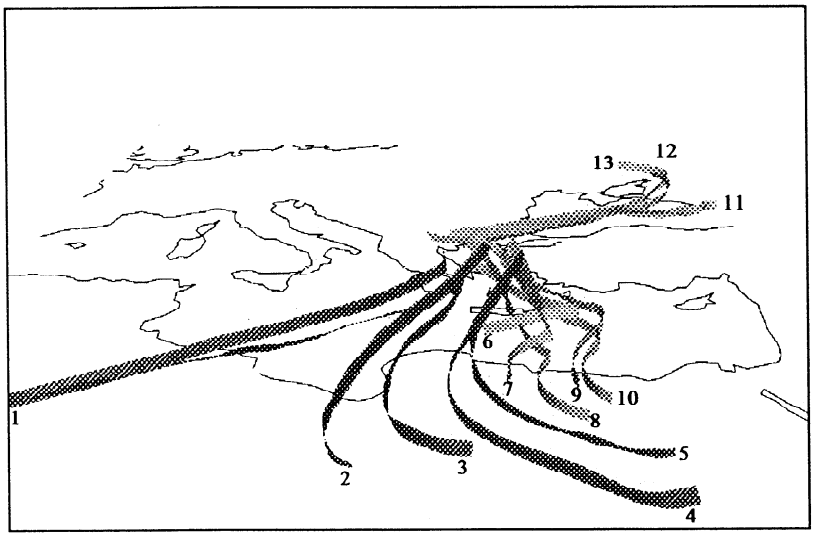

Figure 11. ETA trajectories starting at 0000 UTC October 20, 1994, and ending at 1800 UTC October 21, 1994. Trajectories numbered 1-5 start at about 1.5 km from the Sahara, trajectories 6-10 start at about 150 m, from northeastern Africa, and trajectories 11-13 start at about 150 m from the northern Black Sea.

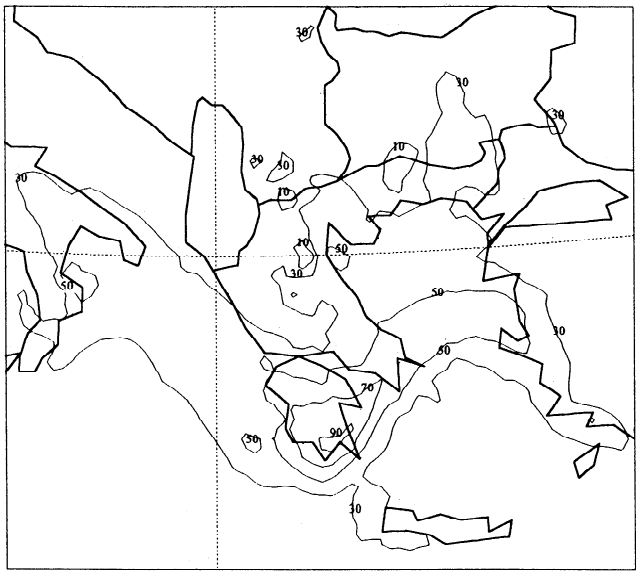

Figure 12. ETA/NMC forecasted total accumulated precipitation from 0600 UTC October 21, to 0600 UTC October 22, 1994 (contour interval of 20 mm).

part of Mediterranean follow the counterclockwise rotation of the low-pressure system over the Aegean Sea, resulting in a strong inflow of air in Northern Greece. This inflow is in good agreement with RAMS results.

The RAMS model simulations are considered as successful in describing the main mesoscale features of the precipitation pattern. The model predicted well the heavy precipitation observed over southern Greece as well as the two regions of heavy precipitation separated by a dry region over northern Greece. The predicted precipitation amounts compared quite well with the observations taking into account that the spatial and temporal variability of the precipitation field is very difficult to be objectively analyzed by a sparse rain gauge network data. The ETA/NMC model succeeded in reproducing the main mesoscale features of the precipitation field due to the high-resolution setup of the model, but its major shortcoming was that it underforecasted the precipitation amounts especially in northern Greece.

Data analysis and model simulations suggest that the main reason for this flooding event in the eastern part of Greece must be mainly due to the orientation of the low-level airflow. More specifically, the boundary layer air masses are fed with moisture which is conveyed by the low-level southwestern flow over the Mediterranean. During this period of the year the sea surface temperature is relatively high and, therefore, the evaporation from the sea surface is enhanced. The moist air masses are deflected upward at the slopes of the mountains over the Greek Peninsula creating enough updraft to initiate free convection. The spatial topographic variations created variations of the convective activity and therefore variations of the spatial distribution of rainfall.

Acknowledgements. The authors greatly acknowledge Craig Tremback and Robert Walko (ASTER Division of Mission Research Corporation) for their helpful suggestions about the RAMS simulations. Acknowledgement is made to the National Center for Atmospheric Research, which is sponsored by the National Science Foundation, for the computing time used in this research (Contract 35081147), and for providing the sounding and surface data used in this study.

References

Avissar, R., and Y. Mahrer, Mapping frost sensitive areas with a three dimensional local scale numerical model, I, Physical and numerical aspects, *J. Appl. Meteorol.*, *27*, 400-413, 1988.

Belair, S., D.L. Zhang, and J. Mailhot, Numerical prediction of the 10-11 June 1985 squall line with Canadian regional finite element model, *Weather Forecast.*, *9*, 157-172, 1994.

Betts, A.K., and M.J. Miller, A new convective adjustment scheme, II, Single column tests using GATE wave, BOMEX and arctic air mass data sets, *Q. J. R. Meteorol. Soc.*, *112*, 693-709, 1986.

Browning, K.A., and C.W. Pardoe, Structure of low-level jet streams ahead of mid-latitude cold fronts, *Q. J. R. Meteorol. Soc.*, *99*, 619-638, 1973.

Chen, C., and W.R. Cotton, The physics of the marine stratocumulus-capped mixed layer, *Boundary Layer Meteorol.*, *25*, 289-321, 1987.

Clark, T.L., and R.D. Farley, Severe downslope windstorm calculations in two and three spatial dimensions using anelastic interactive grid nesting: A possible mechanism for gustiness, *J. Atmos. Sci.*, *41*, 329-350, 1984.

Ducrocq, V., and P. Bougeault, Simulation of an observed squall line with a meso-β scale hydrostatic model, *Weather Forecast.*, *10*, 380-399, 1995.

Hemler R.S., F.B. Lipps, and B.B. Ross, A simulation of a squall line using a nonhydrostatic cloud model with a 5-km horizontal grid, *Mon. Weather Rev.*, *119*, 3012-3033, 1991.

Hobbs, P.V., T.J. Matejka, P.H. Herzegh, J.D. Locatelli, and R.A. Houze, The mesoscale and microscale structure and organization of clouds and precipitation in mid-latitude cyclones, I, A case study of a cold front, *J. Atmos. Sci.*, *37*, 568-596, 1980.

Janjic, Z. I., The step mountain ETA coordinated model: Further developments of the convection, viscous sublayer, and turbulence closure schemes, *Mon. Weather Rev.*, *122*, 927-945, 1994.

Klemp, J.B., and D.K. Lilly, Numerical simulation of hydrostatic mountain waves, *J. Atmos. Sci.*, *35*, 78-107, 1978.

Kotroni, V., and K. Lagouvardos, Low-level jet streams associated with atmospheric cold fronts - seven case studies from the FRONTS87 experiment, *Geophys. Res. Lett.*, *20*, 1371-1374, 1993.

Kotroni, V., Y. Lemaitre, and M. Petitdidier, Dynamics of low-level jet observed during the FRONTS 87 experiment, *Q. J. R. Meteorol. Soc.*, *120*, 277-303, 1994.

Mahrer, Y. and R.A. Pielke, A numerical study of the airflow over irregular terrain, *Beitr. Phys. Atmos.*, *50*, 98-113, 1977.

McCumber, M.C., and R.A. Pielke, Simulation of the effects of surface fluxes of heat and moisture in a mesoscale numerical model, I, Soil layer, *J. Geophys. Res.*, *86*, 9929-9938, 1981.

Mellor, G.L., and T. Yamada, Development of a turbulence closure model for geophysical fluid problems, *Rev. Geophys.*, *20*, 851-875, 1982.

Mesinger, F., Z.I. Janjic, S. Nickovic, D. Gavrilov, and D.G. Deaven, The step mountain coordinate: Model description and performance for cases of Alpine lee cyclogenesis and for a case of Appalachian redevelopment, *Mon. Weather Rev.*, *116*, 1493-1518, 1988.

Pielke, R.A, et al., A comprehensive meteorological modeling system - RAMS, *Meteorol. Atmos. Phys.*, *49*, 69-91, 1992.

Ross, B.B., The role of low-level convergence and latent heating in a

simulation of observed squall line formation, *Mon. Weather Rev., 115*, 2298-2321, 1987.

Snook, J.S., and R. A. Pielke, Diagnosing a Colorado heavy snow event with a nonhydrostatic numerical model structure for operational use, *Weather Forecast., 10*, 261-285, 1995.

Thorpe, A.J. and S.A. Clough, Mesoscale dynamics of cold fronts: Structures described by dropsoundings in FRONTS 87, *Q. J. R. Meteorol. Soc., 117*, 903-941, 1991.

Tremback, C. J., Numerical simulation of a mesoscale convective complex: Model development and numerical results, Ph.D. dissertation, Atmos. Sci. Paper 465, Colo. State Univ., Dep. of Atmos. Sci., Fort Collins, Co 100., 1990.

Tripoli, G.J., and W.R. Cotton, A numerical investigation of several factors contributing to the observed variable intensity of deep convection over south Florida, *J. Appl. Meteorol., 19*, 1037-1063, 1980.

Tripoli, G.J., and W.R. Cotton, The Colorado State University three-dimensional cloud/mesoscale model-1982, I, General theoretical framework and sensitivity experiment, *J. Rech. Atmos., 16*, 185-220, 1982.

Warner, T.L., and N.L. Seaman, A real-time mesoscale numerical weather prediction system used for research, teaching, and public service at the Pennsylvania State University, *Bull. Am. Meteorol. Soc., 71*, 705-792, 1990.

Whitaker, J.S., L.W. Uccellini, and K.F. Brill, A model based diagnostic study of the rapid development phase of the President's day cyclone, *Mon. Weather. Rev., 116*, 2337-2365, 1988.

Zhang, D.L., and J.M. Fritsch, Numerical simulation of the meso-â scale structure and evolution of the 1977 Johnstown flood, I, Model description and verification, *J. Atmos. Sci., 43*, 1913-1943, 1986.

Zhang, D.L., K. Gao, and D.B. Parsons, Numerical simulation of an intense squall line during 10-11 June 1985 PRESTORM, I, Model verification, *Mon. Weather Rev., 117*, 960-994, 1989.

S. Dobricic, G. Kallos, V. Kotroni, K. Lagouvardos, and S. Nickovic, Department of Applied Physics, Laboratory of Meteorology, University of Athens, 33, Ippokratous Str. 10680, Athens, Greece. (e-mail: lagouvar@etesian.meteolab.ariadne-t.gr)

(Received October 12, 1995; revised February 28, 1996;
accepted April 22, 1996.)